Effect of the Thermal Treatment on the Microstructure and Magnetic Property of $Fe_{68}Zr_{20}B_{12}$ Alloy Prepared by Mechanical Alloying

Y.M. Sun, W.Q. Yu and Z. Hua*
College of Physics, Jilin Normal University, Siping, Jilin, 136000, China

(Received July 28, 2010; revised version October 9, 2010; in final form November 3, 2010)

$Fe_{68}Zr_{20}B_{12}$ amorphous alloy prepared by mechanical alloying technique of 60 h of duration was annealed at different temperatures (420–720 °C) during 1 h. Microstructure and magnetic property of as-milled and annealed alloy were investigated by X-ray diffraction, transmission electron microscopy, the Mössbauer spectroscopy and vibrating sample magnetometer techniques. $Fe_{68}Zr_{20}B_{12}$ powders milled during 60 h exhibit amorphous character. After annealing at 420 °C, α-Fe phase precipitates from amorphous matrix. Transmission electron microscopy analysis shows the nucleation and growth of α-Fe grains. The Mössbauer results of the annealed alloy at 670 °C show that the Fe_3B phase precipitates already and there is still remaining amorphous phase. Coercivity increases with increasing annealing temperature, which is closely related to the microstructures after annealing.

PACS: 68.37.Lp, 61.05.Qr

1. Introduction

Since the discovery of FeZrB nanocrystalline alloy, it has attracted a lot of attention owing to its soft magnetic character [1–14]. It is well known that magnetic properties of ferromagnetic materials can be improved by modifying their microstructure. FeZrB amorphous alloys exhibit excellent soft magnetic properties after being annealed under careful conditions, when they reach a nanocrystalline (Nanoperm) microstructure characterized by a nanometric bcc-Fe phase surrounded by a residual amorphous matrix [7]. Low coercivity (H_c) is one of the most important parameters of the excellent soft magnetic properties. Coercivity of FeZrB(Cu) alloy as a function of annealing temperature was investigated over the past several decades [11–14]. However, it is remarkable to note that little attention has been paid for the H_c of FeZrB(Cu) alloy prepared by mechanical alloying (MA). Grain size of α-Fe is one of the most important factors for controlling the soft magnetic properties. Coercivity decreases rapidly with decreasing grain size $D < 100$ nm [15]. Suzuki et al. [16, 17] have shown that the coercivity of Nanoperm type FeZrB(Cu) follows a simpler D^3 power law, which can be found even in the classical composition [18].

MA is considered as a special form of solid-state reaction and can lead to amorphization in a wide composition range [19]. In this work, $Fe_{68}Zr_{20}B_{12}$ amorphous alloy has been prepared by MA successfully and the microstructure after annealing and H_c as a function of annealing temperature are discussed in detail.

2. Experimental details

Sample with nominal composition of $Fe_{68}Zr_{20}B_{12}$ was prepared by MA. Fe, Zr and B powders with purity above 99% were sealed in a cylindrical stainless steel vial under argon atmosphere (99.9%). The milling procedure was carried out in a GN-2 planetary ball mill. The ball-to-powder weight ratio was 30:1. Powders of the alloy were milled for 60 h. After this procedure, the alloy was collected and annealed at 420, 570, 670 and 720 °C during 1 h.

Structural character of the samples was examined by X-ray diffraction (XRD, D/max 2500/PC, using radiation Cu K_α, $\lambda = 1.5406$ Å), transmission electron microscopy (TEM, JEM-2100E, 200 kV) and the Mössbauer spectroscopy. ^{57}Fe Mössbauer spectroscopy was collected on FAST Comtec at room temperature using a conventional constant acceleration type spectrometer with a moving source of ^{57}Co in Pd matrix. Grain size (D) of α-Fe was calculated by the Scherrer formula $D = 0.89\lambda/\beta\cos\theta$ (β indicates the width of half-height diffraction peak, θ is the Bragg angle, λ is X-ray wavelength, D is grain size). The exothermic peaks were measured by differential thermal analysis (DTA, TG/DTA-6300). Magnetic property was measured by vibrating sample magnetometer (VSM, Lake Shore M7407).

* corresponding author; e-mail: huazhong196110@163.com

3. Results and discussion

XRD pattern of $Fe_{68}Zr_{20}B_{12}$ alloy milled during 60 h is shown in Fig. 1. The inset shows the DTA curve of the as-milled alloy. No crystalline peaks were detected in the XRD pattern, which indicates that the alloy milled during 60 h exhibits amorphous character.

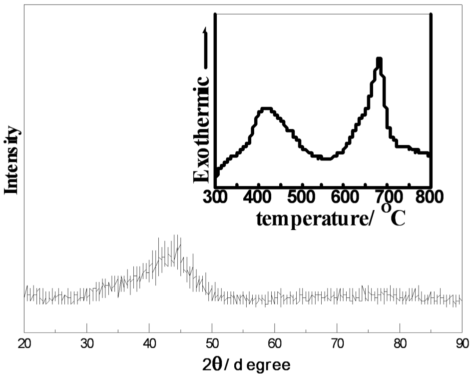

Fig. 1. XRD pattern of $Fe_{68}Zr_{20}B_{12}$ alloy milled during 60 h. The inset shows the DTA curve of $Fe_{68}Zr_{20}B_{12}$ alloy as-milled.

Figure 2 shows the XRD patterns of the annealed alloy at 420, 570, 670 and 720 ℃ during 1 h. Annealing at 420 ℃ induces the precipitation of α-Fe phase from the amorphous matrix and the three peaks of the α-Fe (from left to right) represent (110), (200) and (211) diffraction, respectively. When the annealing temperature increases, more α-Fe crystalline grains precipitate and the diffraction peak intensity increases. The crystalline phases precipitated at the final annealing stage were identified to be α-Fe, Fe_3B and ZrO_2 phases. The grain size (α-Fe) of the alloy annealed at 420, 570, 670 and 720 ℃ was estimated to be about 10.8, 12.4, 19.3 and 31.7 nm, respectively. The grain size (α-Fe) increases with increasing annealing temperature.

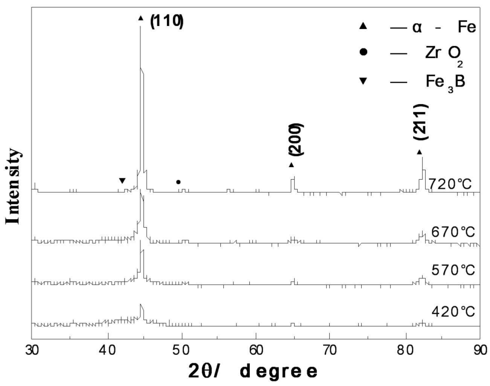

Fig. 2. XRD patterns of $Fe_{68}Zr_{20}B_{12}$ alloy annealed at 420, 570, 670 and 720 ℃.

Figure 3 is the high-resolution TEM image of ZrO_2 of the alloy annealed at 570 ℃. The calculated *d*-space is consistent with the (011) plane of ZrO_2. On the one hand, the oxygen is leaded-in during the process of milling [20]. In addition, the precipitation of ZrO_2 is associated to an internal oxidation process caused by the diffusion of thermally activated oxygen in the as-milled sample during the heat treatment [21].

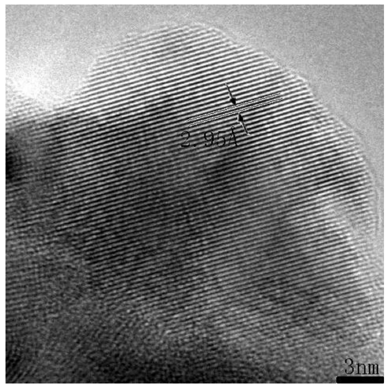

Fig. 3. High-resolution TEM image of $Fe_{68}Zr_{20}B_{12}$ alloy annealed at 570 ℃, showing (011) plane of ZrO_2.

TEM images and high-resolution TEM images of annealed alloys at different temperatures are shown in Fig. 4. The initial nucleation process of crystal grains can be observed in Fig. 4a, that is, for the as-milled alloy annealed at 420 ℃. When the annealing temperature reaches 670 ℃, the grain size increases (Fig. 4b). The high-resolution TEM image of alloy annealed at 720 ℃ (Fig. 4c) is shown in Fig. 4d. The calculated *d*-space is consistent with the value for (110) plane of the α-Fe phase.

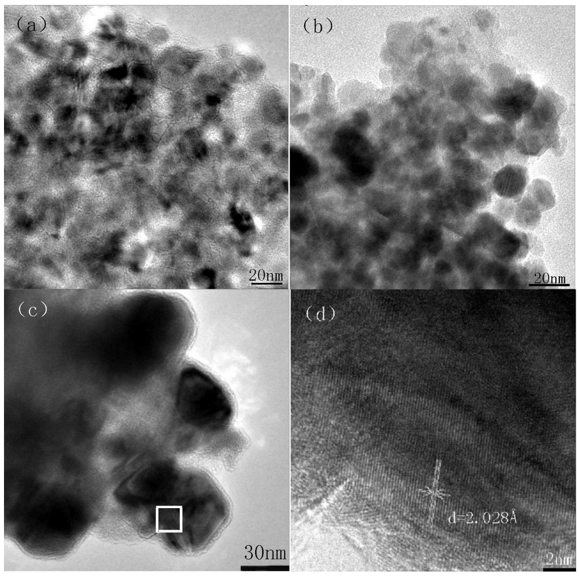

Fig. 4. TEM images of $Fe_{68}Zr_{20}B_{12}$ alloy annealed at 420, 670 and 720 ℃ (a)–(c). The high-resolution TEM image of alloy annealed at 720 ℃ (c) is shown in (d).

The Mössbauer spectrum of the as-milled alloy annealed at 670^{o}C is shown in Fig. 5. Such Mössbauer spectrum shows five sextets and a quadrupole split doublet. The five sextets correspond to α-Fe phase, Fe_3B phase and amorphous phase. The sextet with hyperfine field ($H_{\rm hf}$) = 33.3 T and isomer shift (δ) = -0.02 mm/s corresponds to the α-Fe phase. The sextets with $H_{\rm hf}$ of 29.2, 25.0 and 19.2 T correspond to the tetragonal Fe_3B phase. This means that Fe_3B phase precipitates already when the alloy is annealed at 670 ℃. The grain size distribution of the as-milled alloy annealed at 670 ℃ is shown in Fig. 6. The average grain size is about 11.1 nm. From the XRD analysis of the annealed sample at 670 ℃ one cannot detect the presence of the Fe_3B phase probably due to the small value of the grain size. The quadrupole split doublet corresponds to Fe-rich FeZr amorphous phase [22, 23]. The isomer shift (δ) of quadrupole split doublet is -0.07 mm/s, which is determined by the Zr $\rightarrow$ Fe charge transfer of s-electrons.

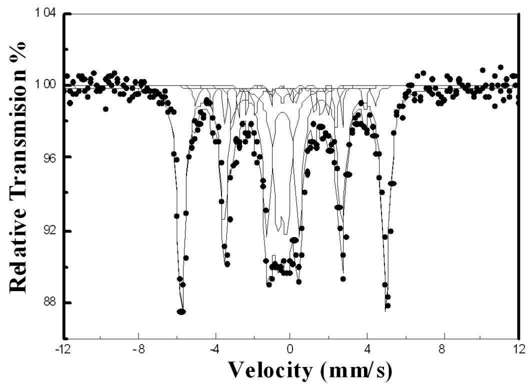

Fig. 5. Mössbauer spectrum of $Fe_{68}Zr_{20}B_{12}$ alloy annealed at 670 ℃.

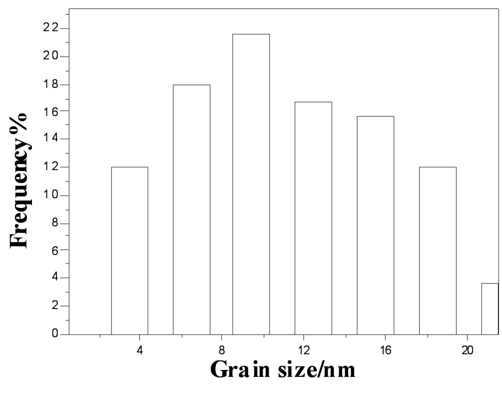

Fig. 6. Grain size distribution of the as-milled alloy annealed at 670 ℃.

Figure 7 shows the variation of coercivity ($H_{\rm c}$) of the as-milled amorphous alloy as a function of the annealing temperature ($T_{\rm a}$). The Mössbauer spectrum indicates that the Fe_3B phase precipitates already, so $H_{\rm c}$ of the alloy annealed at 670 ℃ increases sharply. Due to the precipitations of more Fe_3B and ZrO_2 compounds and the increase of grain size of α-Fe phase, $H_{\rm c}$ of the alloy annealed at 720 ℃ increases continuously, as a probe that the exchange coupling is lost due to that the grain size is comparable to the exchange correlation length.

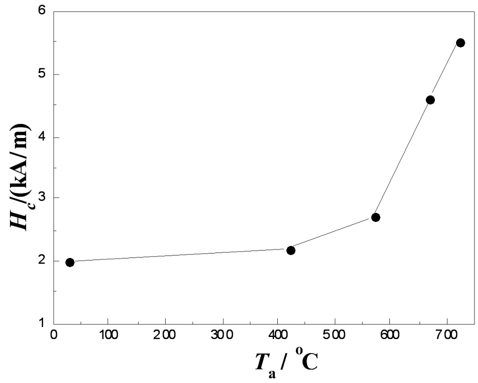

Fig. 7. Coercivity ($H_{\rm c}$) as a function of annealing temperature ($T_{\rm a}$) of the as-milled alloy.

4. Conclusions

We report microstructural analysis and magnetic behaviour of the $Fe_{68}Zr_{20}B_{12}$ alloy prepared by mechanical alloying during 60 h submitted to a post thermal treatment (420–720 ℃ during 1 h). The following aspects can be remarked:

(1) XRD results show that α-Fe phase precipitates from the amorphous matrix when the as-milled alloy is annealed at 420 ℃. Annealing at 720 ℃ leads to the full precipitation of the crystalline phases containing α-Fe, Fe_3B and ZrO_2 phases.

(2) TEM results show that the initial nucleation of crystal is observed when the as-milled alloy is annealed at 420 ℃. Annealing at 670 ℃, the average grain size is about 11.1 nm. The (011) plane of ZrO_2 phase and the (110) plane of α-Fe phase are shown in high-resolution TEM images.

(3) The Mössbauer results of the annealed alloy at 670 ℃ show that the Fe_3B phase precipitates already and there is still remaining amorphous phase.

(4) The Mössbauer spectrum indicates that the Fe_3B phase precipitates already, so $H_{\rm c}$ of alloy annealed at 670 ℃ increases sharply. Due to the precipitations of more Fe_3B and ZrO_2 compounds and the increase of the grain size, $H_{\rm c}$ of $Fe_{68}Zr_{20}B_{12}$ alloy annealed at 720 ℃ increases continuously, as a probe that the exchange coupling is lost due to that the grain size is comparable to the exchange correlation length.

Acknowledgments

This work was funded by Science and Technology Development Project of Siping City (No. 2008023).

References

[1] K. Suzuki, N. Kataoka, A. Inoue, A. Makino, T. Masumoto, *Mater. Trans. JIM* **31**, 743 (1990).

[2] W.S.D. Folly, V.R. Caffarena, R.L. Sommer, J.L. Capitaneo, A.P. Guimarães, *J. Magn. Magn. Mater.* **320**, 358 (2008).

[3] H. Huang, G. Shao, P. Tsakiropoulos, *J. Alloys Comp.* **459**, 185 (2008).

[4] S. Stankov, B. Sepiol, T. Kaňuch, D. Scherjau, R. Würschum, M. Miglierini, *J. Phys., Condens. Matter* **17**, 3183 (2005).

[5] J.S. Garitaonandia, P. Gorria, L. Fernández Barquín, J.M. Barandiarán, *Phys. Rev. B* **61**, 6150 (2000).

[6] A. Makino, K. Suzuki, A. Inoue, Y. Hirotsu, T. Masumoto, *J. Magn. Magn. Mater.* **133**, 329 (1994).

[7] K. Suzuki, A. Makino, A. Inoue, T. Masumoto, *J. Appl. Phys.* **70**, 6232 (1991).

[8] R. Schäfer, C. Stiller, J. Eckert, U. Klement, S. Roth, L. Schultz, *IEEE Magn. Soc.* **32**, 4383 (1996).

[9] C. Stiller, J. Eckert, S. Roth, R. Schäfer, U. Klement, L. Schultz, *J. Non-Cryst. Solids* **205-207**, 620 (1996).

[10] L.K. Varga, D. Kaptás, T. Kemény, *Mater. Sci. Forum* **269-272**, 731 (1998).

[11] P. Marín, C. Gómez-Polo, A. Hernando, *Mater. Sci. Eng. A* **449-451**, 71 (2007).

[12] J.C. Tang, X.Y. Mao, S.D. Li, W.L. Gao, Y.W. Du, *J. Alloys Comp.* **375**, 233 (2004).

[13] A. Makino, T. Bitoh, A. Inoue, T. Masumoto, *J. Appl. Phys.* **81**, 2736 (1997).

[14] A. Ślawska-Waniewska, P. Nowicki, H.K. Lachowicz, P. Gorria, J.M. Barandiarán, A. Hernando, *Phys. Rev. B* **50**, 6465 (1994).

[15] G. Herzer, *J. Magn. Magn. Mater.* **112**, 258 (1992).

[16] K. Suzuki, G. Herzer, J.M. Cadogan, *J. Magn. Magn. Mater.* **177-181**, 949 (1998).

[17] K. Suzuki, J.M. Cadogan, *J. Appl Phys.* **85**, 4400 (1999).

[18] N. Murillo, J. Gonzalez, *J. Magn. Magn. Mater.* **218**, 53 (2000).

[19] N. Schlorke, J. Eckert, L. Schultz, *Mater. Sci. Eng. A* **226-228**, 425 (1997).

[20] Y.J. Liu, I.T.H. Chang, M.R. Lees, *Scr. Mater.* **44**, 2729 (2001).

[21] Y.J. Liu, I.T.H. Chang, *Mater. Sci. Eng. A* **375-377**, 1092 (2004).

[22] A. Grabias, M. Kopcewicz, D. Oleszak, *J. Alloys Comp.* **339**, 221 (2002).

[23] D.Y. Liu, W.S. Sun, A.M. Wang, H.F. Zhang, Z.Q. Hu, *J. Alloys Comp.* **370**, 249 (2004).